Accident Analysis and Prevention 50 (2013) 16–24

Contents lists available at SciVerse ScienceDirect

Accident Analysis and Prevention

journal homepage: www.elsevier.com/locate/aap

# Assessment of injury potential in pediatric bed fall experiments using an anthropomorphic test device

Angela Thompson [a], Gina Bertocci [a,b,c,*], Mary C. Pierce [d]

[a] Mechanical Engineering, University of Louisville, Louisville, KY, USA
[b] Pediatrics, University of Louisville, Louisville, KY, USA
[c] Bioengineering, University of Louisville, Louisville, KY, USA
[d] Children's Memorial Hospital, Northwestern University's Feinberg School of Medicine, Chicago, IL, USA

ARTICLE INFO

*Article history:*
Received 9 February 2012
Received in revised form 23 July 2012
Accepted 6 September 2012

*Keywords:*
Accidental falls
Biomechanics
Child abuse
Injury assessment

ABSTRACT

Falls from beds and other furniture are common scenarios provided to conceal child abuse but are also common occurrences in young children. A better understanding of injury potential in short-distance falls could aid clinicians in distinguishing abusive from accidental injuries. Therefore, this study investigated biomechanical outcomes related to injury potential in falls from beds and other horizontal surfaces using an anthropomorphic test device representing a 12-month-old child. The potential for head, neck, and extremity injuries and differences due to varying impact surfaces were examined. Linoleum over concrete was associated with the greatest potential for head and neck injury compared to other evaluated surfaces (linoleum over wood, carpet, wood, playground foam). The potential for severe head and extremity injuries was low for most evaluated surfaces. However, results suggest that concussion and humerus fracture may be possible in these falls. More serious head injuries may be possible particularly for falls onto linoleum over concrete. Neck injury potential in pediatric falls should be studied further as limitations in ATD biofidelity and neck injury thresholds based solely on sagittal plane motion reduce accuracy in pediatric neck injury assessment. In future studies, limitations in ATD biofidelity and pediatric injury thresholds should be addressed to improve accuracy in injury potential assessments for pediatric short-distance falls. Additionally, varying initial conditions or pre-fall positioning should be examined for their influence on injury potential.



## 1. Introduction

Falls from beds and other furniture are common scenarios provided to conceal child abuse (Duhaime et al., 1992; Leventhal et al., 1993; Strait et al., 1995; Shaw et al., 1997; Scherl et al., 2000). However, short-distance household falls are common occurrences in young children and sometimes result in injury. Because of this, clinicians may have difficulty distinguishing between accidental and inflicted injuries, particularly when the stated scenario is a household fall. Objective assessments of injury potential in these falls may aid clinicians in distinguishing between abusive and accidental injuries. The biomechanics associated with short-distance falls (typically defined as falls from heights less than 4 ft) has been investigated in previous studies, but primarily focused on head injury outcomes (Bertocci et al., 2003, 2004; Prange et al., 2003; Coats and Margulies, 2008; Thompson et al., 2009; Ibrahim and Margulies, 2010). In this study, biomechanical measures relating to head, neck, and extremity injury were examined.

To investigate outcomes relating to injury potential in short-distance household falls, simulations of falls from a horizontal surface (representing a bed or other elevated furniture surface) using a 12-month-old anthropomorphic test device (ATD) were performed. In a clinical study of pediatric falls, rolling off of a bed or other horizontal surface was found to be the most common short-distance fall scenario in infants and toddlers (Thompson et al., 2011). Therefore, in this study, the ATD was positioned to recreate this "rolling off the bed" scenario. The effect of different impact surfaces on injury potential was also examined.

## 2. Methods

### 2.1. Test setup

A child restraint air bag interaction (CRABI) 12-month-old ATD (First Technology Safety Systems, Plymouth, MI) was placed on the edge of a 24 in. (61 cm) high horizontal surface representing a bed,

* Corresponding author at: 500 S. Preston St., University of Louisville, Health Science Research Tower, Rm 204, Louisville, KY 40202, USA. Tel.: +1 502 852 0296.
*E-mail addresses:* angela.thompson@louisville.edu (A. Thompson), g.bertocci@louisville.edu (G. Bertocci), mpierce@luriechildrens.org (M.C. Pierce).

0001-4575/$ – see front matter © 2012 Elsevier Ltd. All rights reserved.
http://dx.doi.org/10.1016/j.aap.2012.09.011

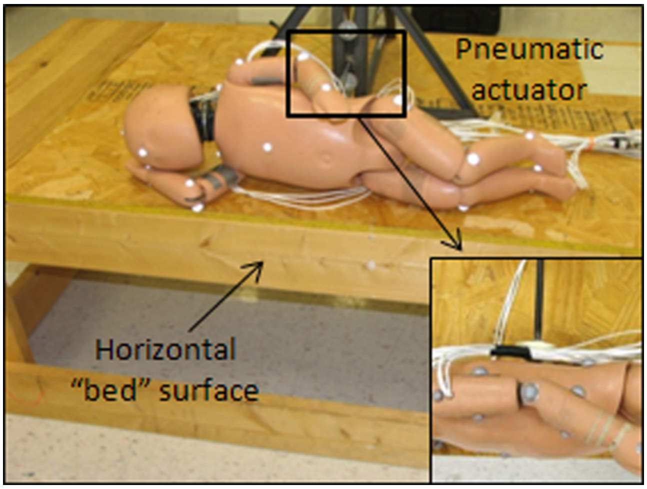


**Fig. 1.** CRABI anthropomorphic test device (ATD) in side-lying initial position for bed fall experiments. The pneumatic actuator (used to deliver a force to the posterior torso of the ATD to push it from the surface) is shown behind the ATD.

couch, or other similar furniture (Fig. 1). The ATD was positioned on the bed in an initial side-lying position and pushed from the surface onto the floor using a pneumatic actuator. The actuator was positioned at the ATD posterior mid-torso (approximately the center of mass location). The actuator provided a consistent initial force just sufficient to push the ATD from the bed surface. Actuator velocity was measured using a motion capture system; peak velocity was 0.95 m/s. Five different impact surfaces were evaluated during the fall experiments. Nine fall trials were performed for each fall scenario based upon a power analysis of prior experiments (Thompson et al., 2009).

*2.1.1. ATD instrumentation*

The CRABI ATD represents a 50th percentile 12-month-old child in terms of overall height (29.7 in./0.75 m) and mass (21.8 lb/9.9 kg), as well as geometric and inertial properties of individual body segments. The ATD was instrumented with tri-axial linear accelerometers (Endevco, Model 7264-2000) located at the center of mass of the head, the overall body center of mass in the torso, and the pelvis. Additionally, two angular rate sensors (ATA Sensors, Model ARS-06) were placed at the center of mass of the head to measure angular velocities in the anterior–posterior (AP) and medial–lateral (ML) directions. Two six-axis load cells (First Technology Safety Systems, Model IF-954) were located at the superior and inferior aspects of the neck (approximately the C1 and C7 vertebrae locations) to measure neck loads. Three uniaxial strain gages and one shear strain gage (Vishay Micro-Measurements, Models CEA-13-125UN-350 and CEA-13-062UV-350) were adhered to each extremity at the longitudinal center of a metal rod representing the humerus or femur. The strains from the three uniaxial gages (120 degrees apart around the rod circumference) were used to determine humerus and femur axial loads and moments, and the strain measured by the shear strain gage was used to determine torsional loads.

Prior to each fall, ATD joint angles were adjusted using a goniometer to ensure repeated positioning for all trials (Table 1). Joints were calibrated to manufacturer specifications: tighten until the friction is just sufficient to support the weight of the limb.

*2.1.2. Impact surfaces*

Five different impact surfaces were evaluated during fall experiments: playground foam, padded carpet, wood, and two types of linoleum flooring (Linoleum A and Linoleum B). These surfaces were selected to simulate some common household surfaces, and also to provide surfaces with a range of stiffnesses. Linoleum A was no-wax self-adhesive vinyl flooring adhered to a wooden platform (1 mm or 0.04 in. thick). The platform (which served as the wood surface) was 183 cm × 183 cm (6 ft × 6 ft) and consisted of 1.9 cm (3/4 in.) plywood covering 5.1 cm × 10.2 cm (2 in. × 4 in.) joists spaced 40.6 cm (16 in.) from the center of one joist to the center of the next. Linoleum B was linoleum tile, 0.32 cm (1/8 in.) thick placed over a concrete floor. The playground foam surface consisted of 61 cm × 61 cm (2 ft × 2 ft) tiles, 5.1 cm (2 in.) thick, and was placed over a concrete subfloor. The carpet was open loop and was 1.3 cm (1/2 in.) thick with 1.0 cm (3/8 in.) thick foam padding and was tacked to the wooden platform.

**Table 1**
Initial ATD joint angles.

| Initial joint angle positions (degrees) | |
|---|---|
| Right shoulder angle | 140° |
| Right elbow angle | 100° |
| Left shoulder angle | 0° |
| Left elbow angle | 150° |
| Hip angle (both) | 150° |
| Knee angle (both) | 150° |

*2.2. Data acquisition and analysis*

A LabView program was developed for data acquisition. Accelerometer, rate sensor, load cell, and strain data were sampled at 10,000 Hz and filtered according to SAE J211 standards. The filter was a 4th order low-pass Butterworth filter. Head acceleration, angular velocity, and neck force data were filtered with a 1000 Hz cut off frequency. Neck moments and femur and humerus strains were filtered with a 600 Hz cutoff. All falls were videotaped (30 Hz) to capture overall fall dynamics.

*2.2.1. Head injury outcomes*

Peak resultant linear head accelerations were determined. Additionally, angular head accelerations were determined by differentiating the measured angular head velocities from the angular rate sensors. Peak angular accelerations, peak change in angular velocities, and impact durations were determined for each fall trial for comparison with published head injury thresholds.

*2.2.2. Neck injury outcomes*

Peak neck loads at the occipital condyles were determined for comparison with proposed injury criteria. Neck loads were transformed from the upper neck load cell to the occipital condyle location in accordance with the procedure described by Eppinger et al. (1999). Also, neck forces and moments were used to calculate neck injury criteria, or $N_{ij}$ values, for combined axial loading and moments as established by the National Highway Traffic Safety Administration (NHTSA) (Eppinger et al., 1999). $N_{ij}$ were calculated as

$$N_{ij} = \frac{F_z}{F_{\text{int}}} + \frac{M_y}{M_{\text{int}}} \tag{1}$$

where the subscripts $ij$ represent the four combined loading mechanisms in the sagittal plane: tension–extension (TE), tension–flexion (TF), compression–extension (CE), and compression–flexion (CF). $F_z$ and $M_y$ are the tension/compression force and flexion/extension moment, respectively, measured at the occipital condyles and $F_{\text{int}}$ and $M_{\text{int}}$ are the critical load values (Table 2).

*2.2.3. Upper and lower extremity injury outcomes*

The measured strains were used to determine bilateral axial compression, bending moment, and torsional arm and leg loads

**Table 2**
Critical intercept values for $N_{ij}$ calculation associated with the 12-month-old CRABI ATD (Eppinger et al., 1999).

| Loading mechanism | Critical load |
|---|---|
| Tension (N) | 1465 |
| Compression (N) | 1465 |
| Flexion (N m) | 43 |
| Extension (N m) | 17 |

(Tuttle, 1981). The axial compression loads ($F$) were calculated using

$$F = AE\left(\frac{\varepsilon_1+\varepsilon_2+\varepsilon_3}{3}\right) \quad (2)$$

and the bending moments ($M$) were calculated using

$$M = \frac{IE(\varepsilon_1-\varepsilon_3)}{\sqrt{3}r\ \cos\theta} \quad (3)$$

and

$$\theta = \tan^{-1}\left[\frac{1}{\sqrt{3}}\left(1-\frac{2(\varepsilon_2-\varepsilon_1)}{(\varepsilon_3-\varepsilon_1)}\right)\right] \quad (4)$$

where $A$ is the cross-sectional area of the humerus/femur surrogate rod, $E$ is the modulus of elasticity, $I$ is the area moment of inertia, $r$ is the radius of the humerus/femur rod, $\theta$ is the angle from one of the gages to the axis about which the bending moment is acting, and $\varepsilon_1$, $\varepsilon_2$, and $\varepsilon_3$ are the maximum, middle, and minimum measured strains, respectively. The torsional loads were calculated directly from the shear strains measured by the shear strain gages using

$$T = \frac{JG\gamma}{r} \quad (5)$$

where $J$ is the polar moment of inertia, $G$ is the shear modulus of the material, $r$ is the radius, and $\gamma$ is the measured shear strain.

*2.2.4. Statistical analysis*

Each of the outcome variables was analyzed separately using one-way analysis of variance (ANOVA) tests to determine if surface type led to significant differences in the outcome measures. Post hoc Tukey tests were also conducted to further examine where significant differences occurred. Statistical significance was set at $p \le 0.05$. SPSS v.12.0.1 was used to perform all statistical analysis.

## 3. Results

### 3.1. Fall dynamics

After actuator initiation, the ATD rolled about the edge of the bed surface (Fig. 2). Initially, the longitudinal (mid-sagittal plane) axis of the body was parallel with the ground. During the fall, the ATD continued to rotate about its longitudinal axis and impacted the floor surface on its side with the head in a leading position (feet elevated above the floor at the time of impact). The head and left shoulder of the ATD impacted the floor surface at approximately the same time. After the initial impact with the floor, the ATD rebounded upward off the floor before finally coming to rest.

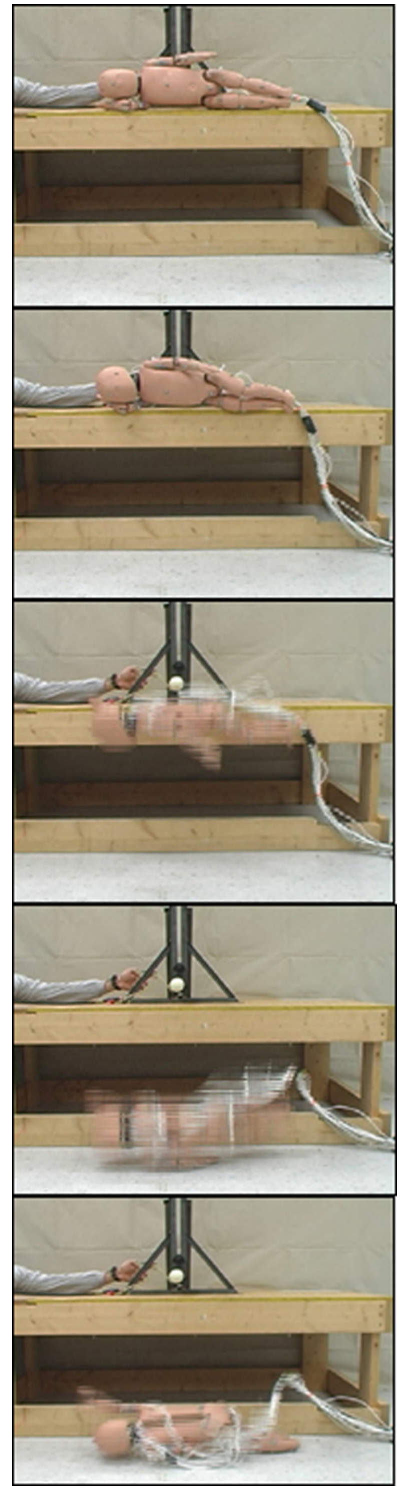

**Fig. 2.** Image sequence of a representative fall onto the Linoleum B impact surface.

### 3.2. Head injury outcome measures

The mean peak resultant linear head acceleration across all surfaces was 135.6 g (Fig. 3). Representative time history curves for falls onto the various tested surfaces are shown in Fig. 4. Falls onto Linoleum B over concrete produced the greatest values, with a maximum of 423.3 g. Mean peak linear head acceleration was significantly greater for falls onto Linoleum B over concrete than all other surfaces ($p < 0.001$). Additionally, mean peak linear head acceleration for falls onto the wood impact surface was significantly greater than those for playground foam ($p = 0.011$) and carpet ($p = 0.043$).

The mean peak angular head accelerations across all surfaces were 3675 rad/s$^2$ and 6172 rad/s$^2$ in the AP and ML directions, respectively (Fig. 5). Peak angular head accelerations were generally greater in the ML direction than in the AP direction. The greatest peak ML angular head acceleration was 11,730 rad/s$^2$ and occurred in a fall onto linoleum B over concrete. As with linear

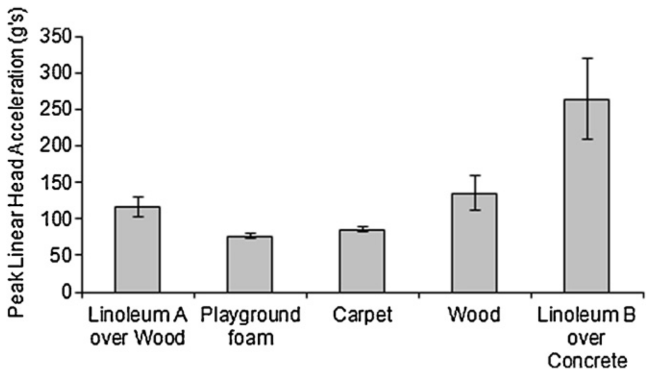


**Fig. 3.** Peak resultant linear head acceleration for falls onto various surfaces. Error bars represent 95% confidence intervals.

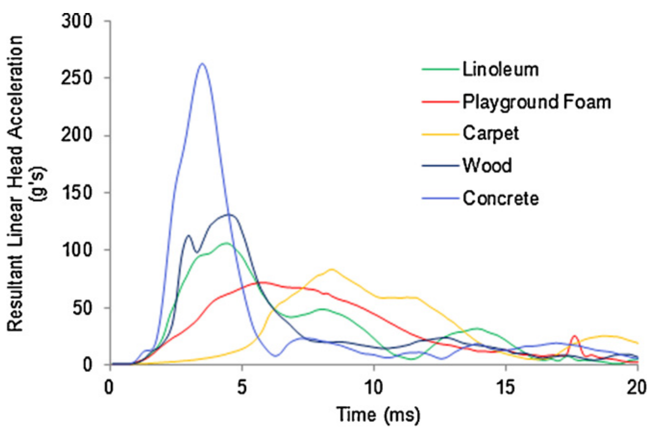


**Fig. 4.** Representative resultant linear head acceleration time histories for falls onto various surfaces.

head accelerations, mean peak AP and ML angular head accelerations were significantly greater for falls onto Linoleum B over concrete than all other surfaces ($p < 0.001$). Additionally, mean peak AP and ML angular head accelerations for wood and Linoleum A over wood were significantly greater than playground foam and carpet surfaces ($p < 0.001$). Mean peak AP angular head acceleration for wood was significantly greater than those for Linoleum A over wood ($p = 0.007$), playground foam ($p < 0.001$), and carpet ($p < 0.001$). Mean peak AP angular head acceleration for falls onto Linoleum A over wood was significantly greater than those for playground foam and carpet ($p < 0.001$). ML peak angular head

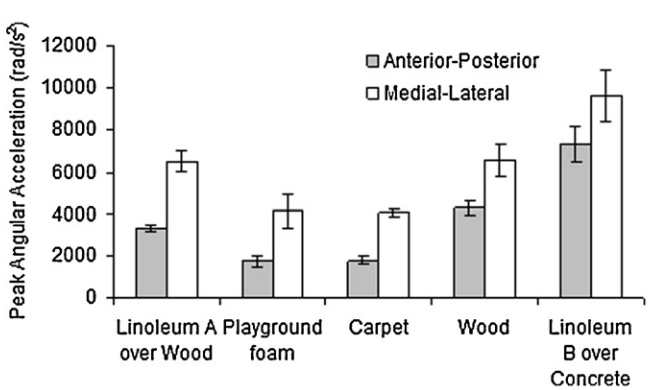


**Fig. 5.** Peak angular head acceleration in the anterior–posterior and medial–lateral directions for falls onto various surfaces. Error bars represent 95% confidence intervals.

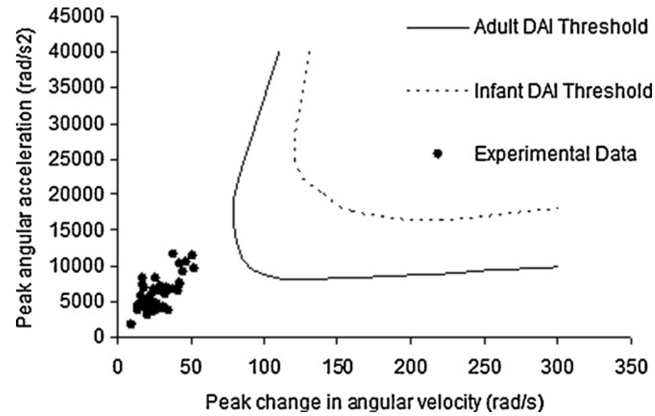


**Fig. 6.** Peak medial–lateral angular head accelerations and peak change in angular velocity: experimental data compared to thresholds for moderate to severe diffuse axonal injury (DAI) (Margulies and Thibault, 1992). Thresholds shown are for an infant and adult with 500 g and 1067 g brain mass, respectively.

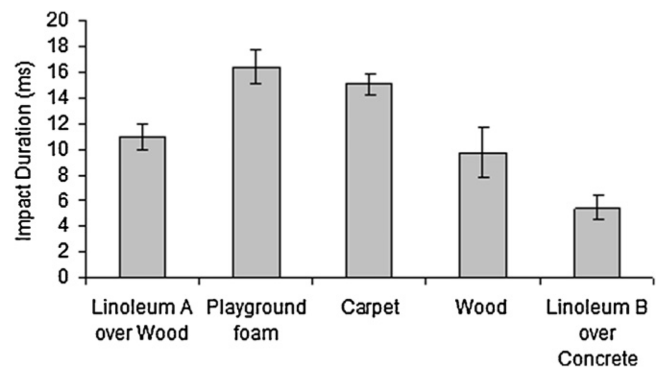


**Fig. 7.** Head impact durations for falls onto various surfaces. Error bars represent 95% confidence intervals.

accelerations have been plotted along with peak change in angular velocity for comparison with proposed injury thresholds (Fig. 6).

Head impact durations ranged from 2.7–19.1 ms with a mean of 11.5 ms (Fig. 7). Mean impact duration was significantly shorter for falls onto Linoleum B over concrete than all other surfaces ($p < 0.001$). Further, mean impact durations for falls onto Linoleum A over wood and wood were significantly shorter than those for playground foam and carpet ($p < 0.001$).

### 3.3. Neck injury outcome measures

The mean peak neck axial compression force across all trials was 779 N (Fig. 8). The greatest bending moments occurred in the lateral direction with a mean of 13.4 N m (Fig. 9). Falls onto linoleum B over concrete produced the greatest neck loads in all measured directions. Peak neck loads were as follows: axial compression – 1504 N, flexion – 17.9 N m, extension – 4.2 N m, lateral bending – 19.2 N m, torsion – 4.1 N m. Mean peak neck compression force was significantly greater in falls onto Linoleum B over concrete than Linoleum A over wood ($p = 0.006$), playground foam ($p < 0.001$), and carpet ($p = 0.017$). Mean peak flexion moment was significantly greater in falls onto Linoleum B over concrete than carpet ($p = 0.019$). Mean peak extension moment was significantly greater in falls onto Linoleum B over concrete than falls onto wood ($p = 0.003$) and carpet ($p = 0.002$). No significant differences in lateral bending moments were found between the tested surfaces. Mean peak torsion moments were significantly greater for falls onto Linoleum B over concrete than for Linoleum A over wood ($p = 0.020$) and carpet ($p = 0.002$), and

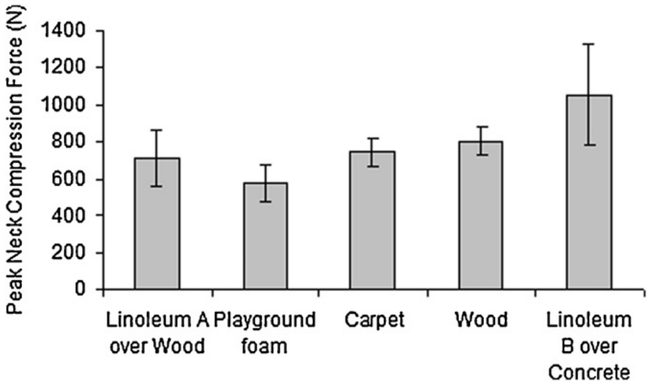


**Fig. 8.** Peak neck compression force for falls onto various surfaces. Error bars represent 95% confidence intervals.

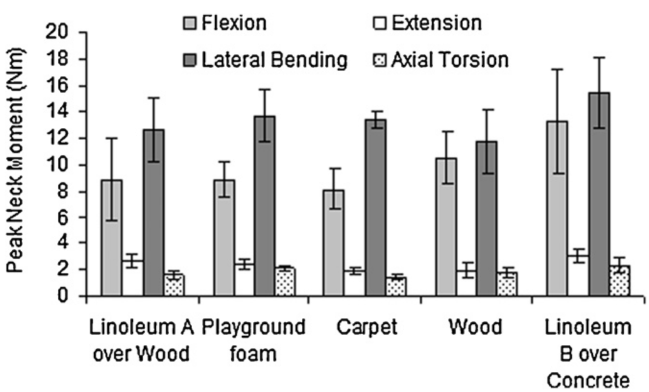


**Fig. 9.** Peak neck moments applied in various directions (flexion, extension, lateral bending, torsion) for falls onto various surfaces. Error bars represent 95% confidence intervals.

for falls onto playground foam compared to falls onto carpet ($p = 0.031$).

$N_{ij}$ calculations were performed to evaluate combined loading mechanisms in the sagittal plane. The greatest $N_{ij}$ values occurred for the compression–flexion loading mechanism ($N_{CF}$) (Fig. 10). The mean $N_{CF}$ value across all surfaces was 0.7. Five of the nine falls onto linoleum B over concrete produced $N_{CF}$ values greater than one (maximum 1.3), and one fall onto the linoleum A over wood surface produced an $N_{CF}$ equal to 1.0.

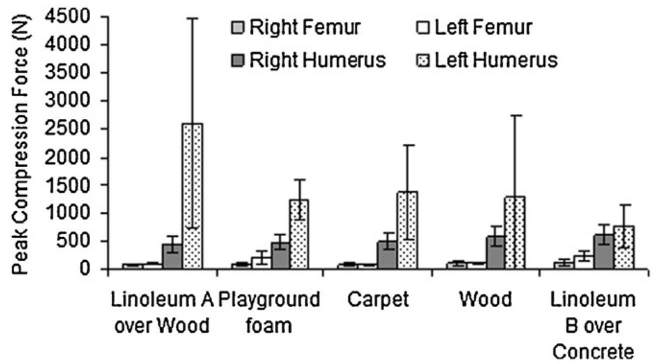


**Fig. 11.** Peak axial compression force for each extremity and for falls onto various surfaces. Error bars represent 95% confidence intervals.

## 3.4. Extremity injury outcome measures

Mean peak compression forces were much greater in the upper extremities than the lower extremities (Fig. 11). The greatest compression forces occurred in the left arm and in falls onto linoleum A over wood (maximum of 6712 N). Unlike head and neck outcome measures, surface trends were less evident in extremity loads. The only significant differences in compression forces across surfaces occurred for the left leg. Mean peak left leg compression force in falls onto Linoleum B over concrete was significantly greater than in falls onto Linoleum A over wood ($p = 0.040$), wood ($p = 0.047$), and carpet ($p = 0.013$).

Mean peak bending and torsion moments were also highest in the left arm (Figs. 12 and 13). The maximum bending moment across all trials was 26.1 N m and occurred in a fall onto linoleum B over concrete. The maximum torsion moment was 23.6 N m and occurred in a fall onto linoleum A over wood. Right leg mean peak bending moment was significantly lower in falls onto Linoleum B over concrete than wood ($p = 0.020$), playground foam ($p = 0.012$), and carpet ($p = 0.040$). Additionally, left leg peak bending moment was significantly greater in falls onto Linoleum B over concrete than onto Linoleum A over wood ($p = 0.016$) and carpet ($p = 0.001$). Left arm mean peak bending moment was significantly greater in falls onto Linoleum B over concrete than falls onto playground foam ($p = 0.045$) and carpet ($p = 0.022$).

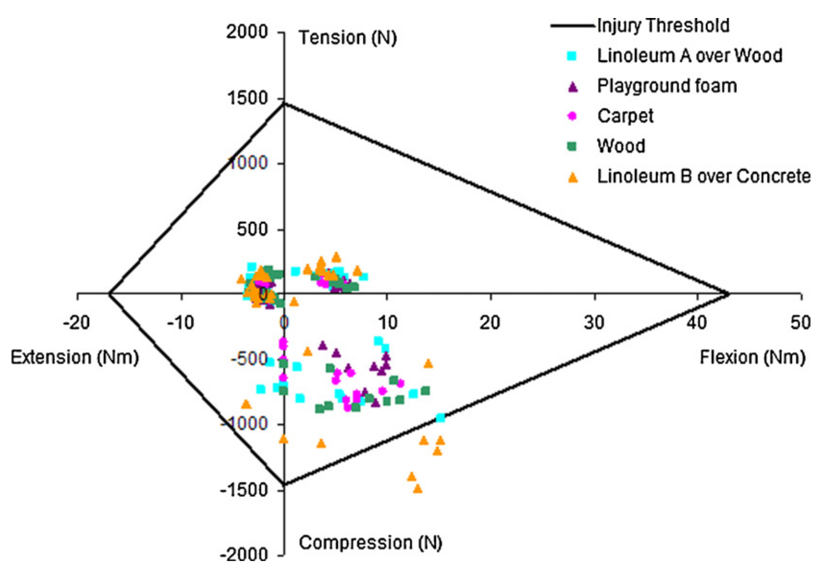


**Fig. 10.** $N_{ij}$ neck injury criteria 12-month-old CRABI threshold and results for falls onto various surfaces.

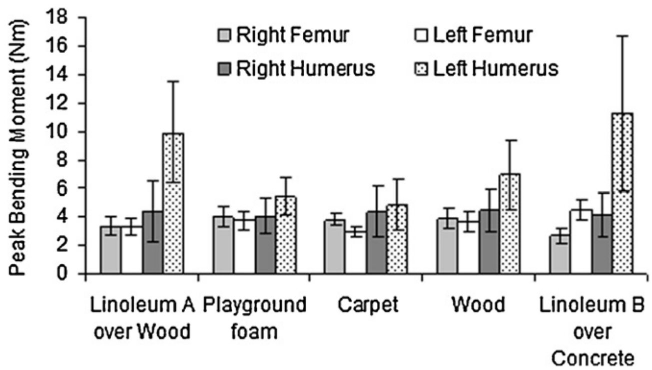


**Fig. 12.** Peak bending moment for each extremity and for falls onto various surfaces. Error bars represent 95% confidence intervals.

## 4. Discussion

### 4.1. Effect of surface

Significant differences in outcome measures were found across the evaluated surfaces. Linoleum B over concrete was associated with significantly greater linear and angular head accelerations and shorter impact durations than all other surfaces. Since greater accelerations and shorter impact durations are generally associated with an increased risk of head injury, the greatest head injury risk would occur in short-distance falls onto Linoleum B over concrete or surfaces with similar properties. Additionally, wood and Linoleum A over wood are associated with a greater risk of head injury than carpet or playground foam surfaces. Similarly, linoleum B over concrete was associated with greater neck forces and moments (and thus a greater risk of neck injury) in these falls. Few differences in extremity loads were found across the various impact surfaces. This is likely due to the high variation in these measures. Nine trials per scenario were conducted based upon a power analysis of head injury outcome measures in previous fall experiments using the CRABI ATD (Thompson et al., 2009). The results of these experiments, however, suggest that a greater number of trials would be necessary for investigation of extremity loads. In future studies, additional fall trials should be conducted to further elicit differences in extremity loads across various impact surfaces.

### 4.2. Head injury potential

To determine the potential for head injury in these falls, the results can be compared to published injury thresholds. Head injury thresholds can be separated into two types: linear

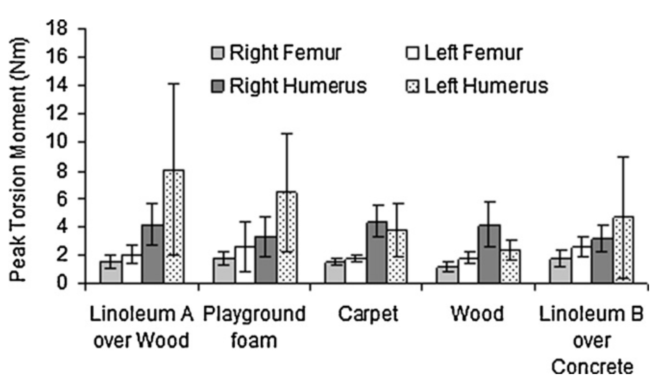


**Fig. 13.** Peak torsional moment for each extremity and for falls onto various surfaces. Error bars represent 95% confidence intervals.

acceleration thresholds (which generally predict potential for focal or contact-type head injuries) and angular or rotational acceleration thresholds (which generally predict potential for inertial or diffuse brain injury). A large range of injury thresholds based on the peak linear acceleration have been proposed for children. Injury assessment reference values have been proposed for the CRABI ATD including a peak linear acceleration limit of 51 g. This limit was chosen to represent less than 5% risk of significant head injury [Nahum and Melvin, 2002]. Sturtz (1980) proposed tolerance limits of 83 g (6–7 year-old children) for impact durations greater than or equal to 3 ms based on reconstructions of pedestrian accidents. Above this acceleration level, abbreviated injury scale (AIS) level 2+ injuries are possible. By using computer simulations to reconstruct free falls resulting in serious head injuries, Mohan et al. (1979) proposed conservative tolerance limits of 200–250 g peak accelerations for children. Others have reported tolerance limits for children ranging from 50 to 200 g where 50 g is the maximum before-injury threshold and 200 g is the threshold for fatal injury (Cory et al., 2001). Peak linear accelerations fell at or below 200 g for all surfaces except Linoleum B over concrete. Linoleum B over concrete produced a maximum linear head acceleration of 423 g. Given the disagreement in thresholds, however, the risk of head injury in these falls is difficult to assess using linear acceleration alone. Additionally, peak g thresholds do not account for the duration of impact. Longer impact durations generally increase the injury risk. Although linoleum B over concrete was associated with the greatest peak linear accelerations, these falls also produced the shortest impact durations (mean duration 5.4 ms).

As with linear head acceleration, many angular acceleration tolerance limits for head injury have been proposed and are often specific to injury type. Additionally, the direction of head rotation is important, as some thresholds differ depending on the direction of the load. The brain is more susceptible to diffuse axonal injury (DAI) under lateral rotation than anterior–posterior rotation (Gennarelli and Meaney, 1996). However, subdural hematomas are more likely to result from rotation in the sagittal plane (anterior–posterior). For this reason, both anterior–posterior and medial–lateral angular accelerations were measured in this study. Reported concussion thresholds are approximately 6500 rad/s$^2$ for a young child (800 g brain mass) and 10,000 rad/s$^2$ for an infant (400 g brain mass) (Ommaya et al., 2002). Similarly, accelerations necessary to cause mild diffuse axonal injury (DAI) have been reported as approximately 18,000 rad/s$^2$ for a young child and 30,000 rad/s$^2$ for an infant. Margulies and Thibault (1992) established tolerance curves for moderate DAI based on peak angular acceleration and peak change in angular velocities (Fig. 6). These curves were derived from a combination of animal experiments, physical models, and analytical model simulations. Duhaime et al. (1987) used a tolerance limit of approximately 35,000 rad/s$^2$ and 40,000 rad/s$^2$ for subdural hematoma (SDH) and DAI, respectively, in an infant with a 500 gram brain mass. Depreitere et al. (2006) proposed a SDH tolerance level of approximately 10,000 rad/s$^2$ for impact durations less than 10 ms based on adult cadaver impact tests. In our study, ML angular accelerations were generally greater than AP angular accelerations (because the ATD landed laterally on the head). The maximum ML angular acceleration across all tested surfaces was 11,730 rad/s$^2$ (occurred in a fall onto linoleum B over concrete). Falls onto surfaces other than linoleum B over concrete produced ML angular head accelerations less than 7400 rad/s$^2$. In comparing our results to proposed thresholds, DAI would not be expected in these falls as all accelerations fell below proposed pediatric thresholds. However, our results suggest that concussion may be possible, particularly for falls onto linoleum B over concrete where several trials exceeded 10,000 rad/s$^2$. The maximum AP angular acceleration was 9322 rad/s$^2$ (occurred in a fall onto Linoleum B over concrete). AP angular accelerations were below

**Table 3**
Fracture thresholds for the adult femur and humerus bones (Levine, 1993).

| Load mechanism | Adult femur thresholds | | Adult humerus thresholds | |
|---|---|---|---|---|
| | Male | Female | Male | Female |
| Compression (kN) | 7.72 | 7.11 | 4.98 | 3.61 |
| Bending moment (N m) | 310 | 180 | 151 | 85 |
| Torque (N m) | 175 | 136 | 70 | 55 |

5000 rad/s$^2$ for all tested surfaces except Linoleum B over concrete. As peak angular accelerations for carpet, playground foam, wood, and Linoleum A over wood fell below proposed SDH thresholds, the potential for SDH in these falls is low. However, peak angular accelerations for falls onto Linoleum B over concrete exceeded the Depreitere adult SDH threshold of 10,000 rad/s$^2$ so there may be a potential for contact SDH in falls onto similar surfaces.

### 4.3. Neck injury potential

Neck injury has been studied much less than head injury, particularly in infants, and thus there are fewer published pediatric neck injury thresholds. One of the most commonly used neck injury assessment thresholds is the $N_{ij}$ criteria. The $N_{ij}$ criteria was developed for use in the automotive industry to assess injury risk in frontal impact motor vehicle impact testing. In this study, compression–flexion was the primary loading mechanism (of the four included in $N_{ij}$). Several falls onto linoleum B over concrete exceeded the threshold and one fall onto linoleum A over wood met the $N_{ij}$ threshold of 1.0. $N_{ij} = 1$ represents a 22% probability of AIS 3 (serious) neck injury, suggesting that serious neck injuries are possible in these falls (Eppinger et al., 1999). These results are particularly concerning since $N_{ij}$ is only calculated for sagittal motion and the primary loading direction in our experiments was in the coronal plane. Additionally, neck injuries have rarely been reported in clinical studies of short-distance falls. This incongruence between biomechanical outcomes and clinical literature highlights concerns regarding the CRABI neck biofidelity or the application of $N_{ij}$ neck injury criteria to pediatric falls. No published injury thresholds were found for lateral bending and torsional neck loading.

### 4.4. Extremity injury potential

In general, peak loads in the upper extremities were greater than those in the lower extremities, and peak loads on the impact (left) side of the body were greater than those on the non-impact (right) side. The fall dynamics were such that the ATD impacted on the left side of the body, causing left arm and leg forces and moments to be greater than those on the right side of the body. Additionally, the ATD's left shoulder impacted the ground at approximately the same time or just after head impact (before the remainder of the body) leading to substantially greater loads in the left arm compared to the other extremities.

Adult bone strength has been well studied, and femur and humerus fracture thresholds are shown in Table 3 (Levine, 1993). Femur and tibia injury criteria for adult ATDs have been established to assess injury risk in automotive impact testing. Femur compression thresholds for the adult Hybrid III 50th percentile (male) and 5th percentile (female) ATDs are 10 kN and 6.8 kN, respectively (Eppinger et al., 1999). Proposed tibia compression thresholds for the adult Hybrid III 50th and 5th percentile ATDs are 35.9 kN and 22.9 kN, respectively. Proposed tibia bending moment thresholds for the adult Hybrid III 50th and 5th percentile ATDs are 225 N m and 115 N m, respectively (Eppinger et al., 1999). Little information is available on pediatric bone strength. A few studies have investigated pediatric femur strength, but no known studies have investigated pediatric humeral strength (Hirsch and Evans, 1965; Currey and Butler, 1975; Chung et al., 1976; Miltner and Kallieris, 1989). Using data from quasi-static bending and compression tests of pediatric femur specimens, Sturtz (1980) estimated the dynamic loads necessary to produce a fracture. This estimation was based on the assumption that dynamic fracture thresholds are 20% higher than quasi-static thresholds. The dynamic bending fracture criteria for a 7 year old and 3.6 year old child were 116–131 N m and 62–73 N m, respectively. Also the dynamic axial (compression) fracture criteria were 1800 and 1000 N for a 6 year old and 3 year old, respectively.

The peak leg compression force, bending moment, and torque across all trials were 647 N, 6.8 N m, and 8.5 N m, respectively. These values fall well below femur fracture thresholds for the adult and the pediatric thresholds proposed by Sturtz. Peak arm compression force, bending moment, and torque across all trials were 6712 N, 26.1 N m, and 23.6 N m, respectively. Upper arm bending moments and torques are below adult injury thresholds. However, our maximum arm compression load exceeds fracture thresholds for the adult (Table 3). As humerus fracture thresholds for the child would likely fall below fracture thresholds for adults, this suggests a risk of humerus fracture due to compressive loading in these falls.

### 4.5. Comparison to other biomechanical studies

Several studies have investigated injury potential in pediatric falls (Bertocci et al., 2003, 2004; Prange et al., 2003; Coats and Margulies, 2008; Thompson et al., 2009; Ibrahim and Margulies, 2010; Thompson et al., 2011). Bertocci et al. (2003) simulated bed falls from a 0.68 m high horizontal surface using a Hybrid II 3-year-old ATD. Although a similar initial position was used by Bertocci et al. as compared to our study, the legs or pelvis of the 3-year-old ATD made first contact with the ground rather than the head. Peak head accelerations were comparable to those measured in our study. Angular head accelerations were not measured. Femur compression and bending loads measured by Bertocci were comparable to those measured in our study. However, torsional loads measured by Bertocci were up to ten times the values measured in this study. This is likely due to the feet-first impact orientation seen in those falls.

Ibrahim and Margulies (2010) simulated falls using an 18-month-old surrogate. The surrogate was dropped from various heights (1–3 ft) onto carpet pad and concrete. The surrogate was initially suspended above the floor in a supine position with the head slightly below the rest of the body (so that the head would impact the ground first). This differs from our study which simulated the entire fall event (rolling off the bed) and did not position the head in a leading position. Peak angular head accelerations reported by Ibrahim and Margulies were more than double those measured in our study. This is likely due to differing skull and neck properties of the surrogates, as well as differences in initial positions. In particular, the CRABI neck is stiffer than Ibrahim's surrogate model (approximately 0.12 N m/degree versus 0.06 N m/degree in flexion and lateral bending).

### 4.6. Comparison to clinical studies

The results of this study are consistent with epidemiological studies of pediatric falls. Two studies of bed falls found no serious head injuries in a combined 512 cases (Helfer et al., 1977; Nimityongskul and Anderson, 1987). There were four skull fractures reported in these studies, but all were of a non-serious nature. Additionally, one humeral fracture and three clavicle fractures were reported by Helfer et al. A study by Tarantino et al. (1999) investigated injuries resulting from short falls (less than 4 ft) in infants less than 10 months of age. Of 167 subjects, 85% had minor or no injury and 15% had significant injuries. Significant injuries included seven long bone fractures (three femur, one humerus, two tibia, and one clavicle), and 18 closed head injuries. Two patients had intracranial hemorrhages but were later determined to be victims of abuse. Hennrikus et al. (2003) found 115 patients with orthopedic injuries resulting from bed falls or falls from other furniture surfaces over a 20-month period. The injuries included fractures and dislocations primarily of the upper extremities. A previous study by Thompson et al. (2011), which reported injuries in 79 clinical cases of household falls, found 6 skull fractures, 9 upper extremity fractures, and 2 lower extremity fractures. This study also reported 2 small isolated SDH. One of the falls that produced a SDH involved a 1-month-old rolling of an 83 cm high bed. However, this child also hit his head on the edge of a humidifier adjacent to the bed. The second case occurred when a 42-month-old child fell rearward from the back of a sofa. In both cases, the children recovered fully. The results of these studies are consistent with our study which suggests a potential for minor head injuries and a low risk for more severe head injuries (such as SDH). Potential for humerus fractures was found in our study, which is consistent with other studies that report injuries to the upper extremities commonly resulting from short-distance falls. However, the risk of femur fracture in this study was very low.

Our findings suggest a potential for neck injuries in bed falls. However, neck injuries have rarely been reported in short-distance falls. Chiaviello et al. (1994) reported that 1 of 69 children who fell down stairs sustained a C2 vertebral fracture. To the authors' knowledge, no neck injuries have been reported from bed falls or other short-distance furniture falls. The neck loads reported in this study should be interpreted with caution as the CRABI neck may be stiffer than an actual 12-month-old child's neck. Additionally, the CRABI neck was designed to investigate injury risk in association with air bag interaction in frontal impact motor vehicle tests. Neck response in lateral bending or axial compression (the two primary loading mechanisms in our simulated falls) were not a biofidelity design requirement of the CRABI ATD.

### 4.7. Limitations

This study has several limitations, some of which are related to the biofidelity of the CRABI ATD. The CRABI neck is likely stiffer than that of a human 12-month-old. A more flexible neck would allow for increased head rotation on impact. Therefore, the head accelerations reported in this study (particularly angular accelerations) may be underestimated. Conversely, increased neck flexibility would likely decrease neck forces and moments. This suggests that the neck loads reported in this study may be overestimated compared to those experienced by a 12-month-old child.

The biofidelity of the CRABI head impact response has been investigated (Irwin and Mertz, 1997; Prange et al., 2004). One study compared the head impact response of a CRABI 6-month-old ATD to that of pediatric cadaveric specimens (ages 1–11 days) in drop tests and found the results to be comparable in vertex, occiput, and forehead impacts (Prange et al., 2004). However, the impact response of the CRABI in lateral impacts was much stiffer than that of the cadaveric specimens. Therefore, the peak linear head accelerations reported in our study may be overestimated compared to what would be experienced by a 12-month-old child.

The CRABI ATD joints (shoulders, elbows, hips, and knees) are primarily limited to rotational motion in the sagittal plane (though a small degree of out of plane motion is possible). As the impact orientation in the simulated falls occurred primarily in the coronal plane, the joint constraints may have affected the fall/impact dynamics and thus the resulting injury outcome measures. Of particular interest are constraints of the left shoulder. With limited shoulder motion outside the sagittal plane, additional loads may have been transferred to the left humerus which may have otherwise been absorbed by shoulder translation in other planes. Therefore, the arm loads in this study may be overestimated. The ATD humeri/femurs were represented by steel and aluminum rods. Metal rods were chosen to facilitate strain measurement but may not accurately represent the deformation characteristics of pediatric bone. This could lead to differences in the loads measured versus those that would be experienced by a human child.

In addition to limitations of the ATD, assessments of injury risk are based on injury criteria that have primarily been determined through scaling of human adult or primate data. This is due to the paucity of information concerning material properties of pediatric tissues and pediatric injury tolerance. Scaling generally accounts for mass differences, but in some cases may account for differences in geometry and material properties. Angular head acceleration thresholds for pediatric brain injury were determined through mass scaling alone. Thibault and Margulies (1998) found that accounting for differences in brain tissue material properties reduced thresholds for concussion, DAI, and SDH. More accurate pediatric injury criteria are needed to improve assessment of injury potential in falls.

It should be noted that only one initial position was simulated in these falls (side-lying to facilitate a rolling motion from the bed surface). Changing initial positions would likely alter the orientation of the ATD upon impact, leading to differences in the injury outcome measures. Additionally, the rate at which the ATD was pushed from the bed surface was held constant. Changes to the initial velocity of the ATD or the "push force" would likely affect the fall dynamics and injury outcome measures. Generally, increases in force would be expected to lead to increases in measured ATD loads. However, initial velocity/force could also affect the orientation of the ATD upon impact. For example, a greater force may lead to more rotation of the ATD thus causing the ATD to land on its back rather than its side. This may reduce the arm loads measured, but increase head accelerations and neck loads (assuming the ATD lands head-first). Any significant deviation from the simulated scenario would require further investigation to more accurately assess injury potential.

## 5. Conclusions

This study investigated biomechanical outcomes related to injury potential in falls from a horizontal surface using an ATD representing a 12-month-old child. The potential for head, neck, and extremity injury was investigated. Significant differences in injury outcome measures for varying impact surfaces were found. Overall, the risk of severe head and extremity injuries in these falls was low onto most surfaces. There is a potential for concussion in the simulated fall scenarios and possibly contact SDH in falls onto surfaces such as linoleum tile over concrete. Fractures, particularly involving the humerus, may also be possible in these falls. Neck injury potential in pediatric falls should be studied further as limitations in ATD biofidelity and neck injury thresholds based solely on sagittal plane motion reduce accuracy in pediatric neck injury assessment. Our findings are a first step toward aiding clinicians in distinguishing between abusive and accidental injuries when the stated cause of the injuries is a short-distance household fall, further highlighting the importance of obtaining a detailed history when assessing compatibility between injury and the stated cause.

## Conflict of interest statement

There are no conflicts of interest for this work.

## Acknowledgments

This research was funded by the University of Louisville Grosscurth Biomechanics Endowment Fund and by the Department of Justice (DOJ), Office of Juvenile Justice and Delinquency Prevention (Award # 2009-DD-BX-0086). The opinions expressed herein are those of the authors and not necessarily those of DOJ.

## References

Anon., 2003. Instrumentation for impact test part 1 – electronic instrumentation. SAE J211.
Bertocci, G.E., Pierce, M.C., Deemer, E., Aguel, F., Janosky, J.E., Vogeley, E., 2003. Using test dummy experiments to investigate pediatric injury risk in simulated short-distance falls. Archives of Pediatrics and Adolescent Medicine 157, 480–486.
Bertocci, G.E., Pierce, M.C., Deemer, E., Aguel, F., Janosky, J.E., Vogeley, E., 2004. Influence of fall height and impact surface on biomechanics of feet-first free falls in children. Injury 35, 417–424.
Chiaviello, C.T., Christoph, R.A., Bond, G.R., 1994. Stairway-related injuries in children. Pediatrics 94 (5), 679–681.
Chung, S.M.K., Batterman, S.C., Brighton, C.T., 1976. Shear strength of the human femoral capital epiphyseal plate. The Journal of Bone and Joint Surgery 58A (1), 94–103.
Coats, B., Margulies, S.S., 2008. Potential for head injuries in infants from low-height falls. Journal of Neurosurgery: Pediatrics 2, 321–330.
Cory, C.Z., Jones, M.D., James, D.S., Leadbeatter, S., Nokes, L.D.M., 2001. The potential and limitations of utilizing head impact injury models to assess the likelihood of significant head injury in infants after a fall. Forensic Science International 123, 89–106.
Currey, J.D., Butler, G., 1975. The mechanical properties of bone tissue in children. The Journal of Bone and Joint Surgery 57A (6), 810–814.
Depreitere, B., Van Lierde, C., Vander Sloten, J., Van Audekercke, R., Van Der Perre, G., Plets, C., Goffen, J., 2006. Mechanics of acute subdural hematomas resulting from bridging vein rupture. Journal of Neurosurgery 104, 950–956.
Duhaime, A.-C., Gennarelli, T.A., Thibault, L.E., Bruce, D.A., Margulies, S.S., Wiser, R., 1987. The shaken baby syndrome: a clinical, pathological, and biomechanical study. Journal of Neurosurgery 66, 409–415.
Duhaime, A.C., Alario, A.J., Lewander, W.J., Schut, L., Sutton, L.N., Seidl, T.S., Nudelman, S., Budenz, D., Hertle, R., Tsiaras, W., Loporchio, S., 1992. Head injury in very young children: mechanisms, injury types, and ophthalmologic findings in 100 hospitalized patients younger than 2 years of age. Pediatrics 90 (2), 179–185.
Eppinger, R., Sun, E., Bandak, F., Haffner, M., Khaewpong, N., Maltese, M., Kuppa, S., Nguyen, T., Takhounts, E., Tannous, R., Zhang, A., Saul, R., 1999. Development of Improved Injury Criteria for the Assessment of Advanced Automotive Restraint Systems – II. National Highway Traffic Safety Administration, U.S. Department of Transportation.
Gennarelli, T.A., Meaney, D.F., 1996. Mechanisms of primary head injury. In: Wilkins, R.H., Renachary, S.S. (Eds.), Neurosurgery. Mc-Graw Hill, New York, pp. 2611–2621.
Helfer, R.E., Slovis, T.L., Black, M., 1977. Injuries resulting when small children fall out of bed. Pediatrics 60 (4), 533–535.
Hennrikus, W.L., Shaw, B.A., Gerardi, J.A., 2003. Injuries when children reportedly fall from a bed or couch. Clinical Orthopaedics and Related Research 407, 148–151.
Hirsch, C., Evans, F.G., 1965. Studies on some physical properties of infant compact bone. Acta Orthopaedica Scandinavica 35, 300–313.
Ibrahim, N.G., Margulies, S.S., 2010. Biomechanics of the toddler head during low-height falls: an anthropomorphic dummy analysis. Journal of Neurosurgery: Pediatrics 6, 57–68.
Irwin, A.L., Mertz, H.J., 1997. Biomechanical bases for the crabi and hybrid III child dummies. Child Occupant Protection.
Leventhal, J.M., Thomas, S.A., Rosenfield, N.S., Markowitz, R.I., 1993. Fractures in young children: distinguishing child abuse from unintentional injuries. American Journal of Diseases of Children 147, 87–92.
Levine, R., 1993. Injury to the extremities. In: Nahum, A.M., Melvin, J.W. (Eds.), Accidental Injury: Biomechanics and Prevention. Springer-Verlag, New York, NY, pp. 460–491.
Margulies, S.S., Thibault, L.E., 1992. A proposed injury tolerance criterion for diffuse axonal injury in man. Journal of Biomechanics 25 (8), 917–923.
Miltner, E., Kallieris, D., 1989. Quasi-static and dynamic bending tests of the infantile thigh in order to produce a femur fracture. Zeitschrift fur Rechtsmedizin 102, 535–544.
Mohan, D., Bowman, B.M., Snyder, R.G., Foust, D.R., 1979. A biomechanical analysis of head impact injuries to children. Journal of Biomechanical Engineering 101, 250–260.
Nahum, A., Melvin, J., 2002. Accidental Injury: biomechanics and prevention. Springer, New York.
Nimityongskul, P., Anderson, L.D., 1987. The likelihood of injuries when children fall out of bed. Journal of Pediatric Orthopedics 7, 184–186.
Ommaya, A.K., Goldsmith, W., Thibault, L., 2002. Biomechanics and neuropathology of adult and paediatric head injury. British Journal of Neurosurgery 16 (3), 220–242.
Prange, M.T., Coats, B., Duhaime, A.-C., Margulies, S.S., 2003. Anthropomorphic simulations of falls, shakes, and inflicted impacts in infants. Journal of Neurosurgery 99, 143–150.
Prange, M.T., Luck, J.F., Dibb, A., Van Ee, C.A., Nightingale, R.W., Myers, B.S., 2004. Mechanical properties and anthropometry of the human infant head. Stapp Car Crash Journal 48, 279–299.
Scherl, S.A., Miller, L., Lively, N., Russinoff, S., Sullivan, C.M., Tornetta, P., 2000. Accidental and nonaccidental femur fractures in children. Clinical Orthopaedics and Related Research 376, 96–105.
Shaw, B.A., Murphy, K.M., Shaw, A., Oppenheim, W.L., Myracle, M.R., 1997. Humerus shaft fractures in young children: accident or abuse? Journal of Pediatric Orthopedics 17 (3), 293–297.
Strait, R.T., Siegel, R.M., Shapiro, R.A., 1995. Humeral fractures without obvious etiologies in children less than 3 years of age: when is it abuse? Pediatrics 96 (4), 667–671.
Sturtz, G., 1980. Biomechanical data of children. In: 24th Stapp Car Crash Conference, Paper No. 801313, SAE, Warrendale, PA.
Tarantino, C.A., Dowd, M.D., Murdock, T.C., 1999. Short vertical falls in infants. Pediatric Emergency Care 15 (1), 5–8.
Thibault, K.L., Margulies, S.S., 1998. Age-dependent material properties of the porcine cerebrum: effect on pediatric inertial head injury criteria. Journal of Biomechanics 31, 1119–1126.
Thompson, A., Bertocci, G., Rice, W., Pierce, M.C., 2011. Pediatric short-distance household falls: biomechanics and associated injury severity. Accident Analysis and Prevention 43, 143–150.
Thompson, A.K., Bertocci, G., Pierce, M.C., 2009. Assessment of head injury risk associated with feet-first free falls in 12-month-old children using an anthropomorphic test device. Journal of Trauma 66 (4), 1019–1029.
Tuttle, M.E., 1981. Load measurement in a cylindrical column or beam using three strain gages. Experimental Techniques 5 (4), 19–20.